

Synthesis and Characterization of Lamellar LiCoO₂ as Cathode Materials for Lithium-Ion Batteries

Zhaorong Chang^{*1}, Zhongjun Chen¹, Hongwei Tang¹, Xiao Zi Yuan² and Haijiang Wang²

¹College of Chemistry and Environmental Science, Henan Normal University, Xinxiang 453007, P.R. China

²Institute for Fuel Cell Innovation, National Research Council of Canada, Vancouver, BC, Canada V6T 1W5

Received: February 08, 2009, Accepted: September 27, 2009

Abstract: Lamellar LiCoO₂ cathode material has been prepared using the co-precipitation method. The synthesized LiCoO₂ powder is characterized by X-ray diffraction (XRD) and scanning electron microscope (SEM). The XRD studies show that the layered material has a α -NaFeO₂ structure with high crystallinity and property of high direction-oriented growth. The SEM confirms that the synthesized LiCoO₂ powder is laminated with its shape similar to the layered structure of the natural shells. At a current of 0.2C rate and 3 - 4.2 V, the initial charge and discharge capacity of 156 and 145mAh·g⁻¹ can be obtained. The capacity of 143mAh·g⁻¹ is retained at the end of 30 charge-discharge cycles with the capacity retention of 99%. The charge-discharge curves at various rates have demonstrated that the laminated LiCoO₂ powders have an excellent rate performance and cycling stability.

Keywords: layered structure; LiCoO₂; cathode material

1. INTRODUCTION

Currently LiCoO₂ is still a major cathode material in the lithium-ion batteries market due to its advantages, such as high operating voltage, high energy density, good cyclic performance, small self-discharge, and no memory effect. Although LiCoO₂ cathode material for Li-ion secondary battery has been widely used, there are still many reports [1] [2] [3] [4] [5] investigating new methods to improve the performance of the material by changing the crystallinity, morphology, and particle size. To date, the commonly used methods include co-precipitation, sol-gel, hydrothermal synthesis, and emulsion drying [6-10].

It has been demonstrated that the slow solid-state diffusion of Li⁺ cations within the electrode materials is the main factor that limits the rate discharge capability of the material [11-12]. Therefore, the shape, size, porosity, agglomeration and growth orientation of the particles will greatly affect the mechanical stress and the Li⁺ diffusion of the material [13-14]. In order to accelerate Li⁺ diffusion, reduce Li⁺ diffusion distance, and increase the surface area of the material, nanostructured LiCoO₂ powders were synthesized for the cathode [15-16]. Compared with the conventional LiCoO₂ powder, nanostructured LiCoO₂ powder can achieve a fast

solid-state diffusion and improved discharge capacity, but it shows a rapid capacity decay and poor cyclic performance. In addition, it is difficult to synthesize nanostructured LiCoO₂ powder due to the harsh synthetical conditions and complicated procedures. To further improve the performance of LiCoO₂, it is necessary to investigate new approaches to synthesize high performance LiCoO₂ material.

Recently, inspired from the natural biological structure, the bio-concepts were introduced to the material research. The laminated materials in structure are quite similar to the shells of the seashell animals. These materials have been extensively used in metallurgy and ceramic because of their unique structures and properties [17]. However, the synthesis and characterization of laminated LiCoO₂ powder as cathode materials for lithium-ion batteries have not been reported thus far. In this paper, we propose a new method in preparing the laminated LiCoO₂ powder. Preliminary results including structure, morphology, and electrochemical properties are presented.

2. EXPERIMENTAL

The procedures for preparing the LiCoO₂ precursor are as follows. The stoichiometric amounts of CoSO₄·7H₂O was dissolved in distilled water, and the concentration of the metal sulfate was

*To whom correspondence should be addressed: Email: czt_56@163.com
Phone: +86-373-3326544 Fax: +86-373-3326544

1.65 mol L⁻¹. The aqueous solution was precipitated by adding NH₄OH, Na₂CO₃ and NaOH solution (about 1~4 mol L⁻¹) under an air atmosphere along with continuous stirring at 50°C for 3h. Then, H₂O₂ (about 0.1 mol L⁻¹) was added to the reaction solution. Subsequent co-precipitation mixtures were stirred continuously about 3h after the reaction ceased. Finally, pure precursor was obtained from the co-precipitation mixtures through coagulation by adding polyacrylamide, filtrating with pressure (20MPa), drying (120°C, 2h), grinding, washing, and drying (120°C, 2h).

Synthesis of laminated LiCoO₂ was carried out using a solid state reaction. The obtained precursor powder was mixed with 5% excess of LiNO₃ (The excessive amount of Li salts was to compensate possible Li loss during the calcination). The mixtures were initially heated to 300°C for 3 h, and then 600°C for 5h. Finally, and they were calcined at 800 °C for 20 h in air. The heating rate was fixed at 240 °C h⁻¹ for all the temperature settings. After the heating, the resulting powders were cooled to ambient temperature.

Thermogravimetric analysis (TGA) and Differential scanning calorimetry (DSC) were carried out on a simultaneous thermal analysis apparatus (NETZSCH STA409 PC/PG) to determine the sintering temperature. The mixture was heated from room temperature to 900 °C at a heating rate of 4 °C min⁻¹. The measurement was performed in nitrogen flow using α -Al₂O₃ as the reference material.

To investigate the crystal structure, the obtained powders were analyzed by X-ray diffraction (XRD) using a D8 X diffractometer (Germany, Bruker) employing Cu-K α radiation. The scan data were collected in the 2 θ range of 10 to 80°. The step size was 0.026° with a counting time of 3 seconds. The morphology and particle size of the prepared powders were also observed using scanning electron microscopy (SEM—XL30).

Slurries containing 85 wt.% of the active material of LiCoO₂, 5 wt.% polyvinylidene fluoride dissolved in *n*-methyl-2-pyrrolidinone, and 10 wt.% acetylene black were spread evenly on a piece of aluminum foil. The sheet was then dried at 120°C for 10 hours and pressed into round slice as the cathode. In an Ar-filled glove box, button cells (CR2025) were assembled with metallic Li as the counter electrode, Celgard 2400 as the separator, and 1 mol L⁻¹ of LiPF₆ in ethylene carbonate and diethyl carbonate (1:1, v/v) as the electrolyte solution. The cells were cycled between 3.0V and 4.2V versus Li/Li⁺ galvanostatically (0.2C, 1C, 2C, 5C rate) on a Land CT2001A battery tester (China, Wuhan Jinnuo Electronics Co. Ltd.) at 25±1°C.

3. RESULTS AND DISCUSSION

3.1. TG--DSC analysis

In order to find a proper temperature range for the reaction, TG/DSC analysis was carried out. Figure 1 shows the TG/DSC curves of the mixture of the precursor and LiNO₃. It is observed that there is a slight weight loss between 100°C and 160°C, which is attributed to the evaporation of water. In the range of 250°C to 600°C, there is one obvious weight loss in the TG curve and there are two pronounced endothermic peaks in the corresponding DSC curve. The first endothermic peak is around 260°C corresponding to the melting process of LiNO₃ (the melting point of LiNO₃ is 260°C). At 260°C, LiNO₃ starts to melt and permeate into the precursor surface and inside. The second endothermic peak at 360°C in the DSC curve relates to the decomposition of LiNO₃. Corre-

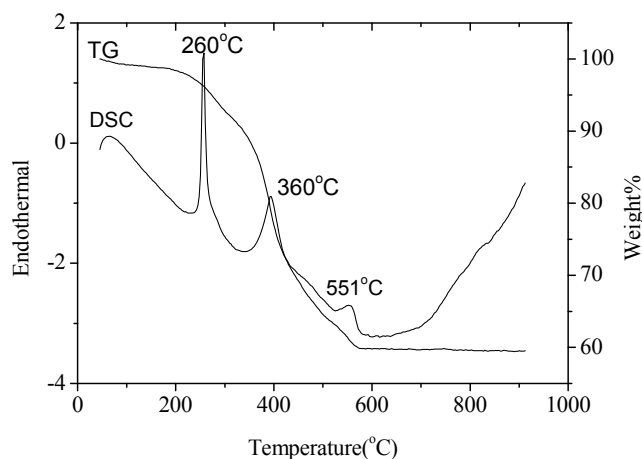


Figure 1. The TG/DSC curves for the mixture of the precursor and LiNO₃.

spondingly, there is a massive weight loss between 300°C and 560°C in the TG curve, which indicates that the reaction of the precursor and LiNO₃ occurs at this temperature range. At 551°C, a broad and weak endothermic peak is seen in the DSC curve, which is attributed to the crystal lattice transformation. When the temperature is higher than 560°C, the TG curve remains constant, and there is no obvious exothermic or endothermic peak in the corresponding DSC curve, which indicates that relative stable LiCoO₂ has been formed. Based on the thermal analysis, it is possible to synthesize the laminated or layered LiCoO₂ cathode material by a three-stage temperature control. First, at 300°C for 3 hours the mixtures of the precursor and LiNO₃ are calcined to melt the lithium salt, which has a low melting point. The molten lithium salt then permeates and diffuses into the inside of the precursor to achieve an even mixture. Then, at 600°C for 5 hours Li⁺ in the molten salt further permeates and diffuses into the inside of the precursor. In the meantime, the reaction occurs and part of the products transforms to the crystal form. Finally, at 800°C for 20 hours the mixtures react completely. The structure further transforms to crystal and the crystal grows with orientation. The desired laminated LiCoO₂ powder with controlled stoichiometry, well-grown structure, and high crystallinity is then obtained.

3.2. XRD analysis of the LiCoO₂ powders

Figure 2 shows the XRD patterns of the LiCoO₂ material obtained by calcining the precursors at 800°C for 20 hours in air. This figure reveals that the synthesized compound has a typical structure of a hexagonal α -NaFeO₂ type with a space group of $R\bar{3}m$. The diffraction peaks are quite intense, indicating a high crystallinity of the synthesized material. No impurity diffraction peaks were observed, representing no impurity phase. As seen from Figure 2, the obvious split of the (006, 102) and (018, 110) peak pairs in the XRD pattern reveals the regular layered structure of the compound [18-19]. As the sizes of Li⁺ and Co³⁺ are very close, cations are easily mixed, worsening the electrochemical properties of the material. Some researchers [20] have used the high integrated intensity ratio of I_{003}/I_{104} to indicate the cation mixing of the material. It has

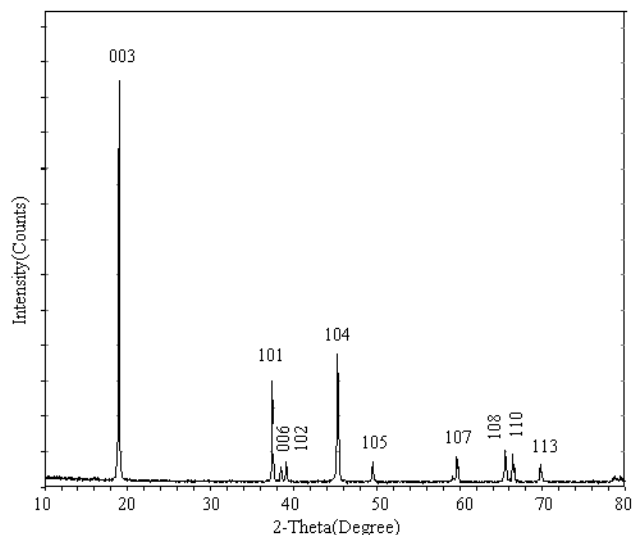


Figure 2. XRD patterns of the laminated LiCoO₂ powder synthesized at 800°C for 20 hours.

Table 1. Calculated structure parameters and the tap-density for the laminated LiCoO₂ powder

Sample	Temperature (°C)	Lattice parameters			I_{003}/I_{104}	R
		$a(\text{Å})$	$c(\text{Å})$	c/a		
LiCoO ₂	800	2.8178	14.0631	4.9908	3.5	0.39

been reported that the smaller the I_{003}/I_{104} value, the higher the disorder. If the I_{003}/I_{104} value is less than 1.2, it means that undesirable cation mixing takes place. Based on Figure 2, the lattice parameters, including a , c , and c/a , I_{003}/I_{104} , and R value of the samples are summarized in Table 1. I_{003}/I_{104} value of 3.5 is observed in the sample, indicating that the cation mixing of the cathode materials, which leads to poor electrochemical performance, was reduced at a satisfactory level [20]. In addition, according to Dahn et al. [21-22], R factor ($R = (I_{102} + I_{006})/I_{101}$) is a main indicator of hexagonal order. The lower the R value, the better the hexagonal order. This material has a low R value of 0.39, which indicates that the lattice has a very good hexagonal order. Based on the XRD analysis the laminated LiCoO₂ powders have a well-ordered hexagonal layered structure with small amounts of cation mixing.

3.3. Morphology of the laminated LiCoO₂ powders

The surface morphology of the laminated LiCoO₂ powders at different magnifications is shown in Figure 3a, 3b and 3c, respectively. It can be clearly seen from Figure 3a and 3b that the synthesized LiCoO₂ powders are about 10 μ m in size, and that the laminated structure of a single particle is regular, which is similar to the shell. Figure 3c shows the SEM image of the laminated LiCoO₂ powders triturated in mortar. As shown in Figure 3c, the triturated particles are uniform and regular with particle size of around 100nm. It is well known that the smaller the electrode material in size, the larger the specific surface area, the more contact with the electrolyte, the less the diffusion distance of Li⁺, and the better the

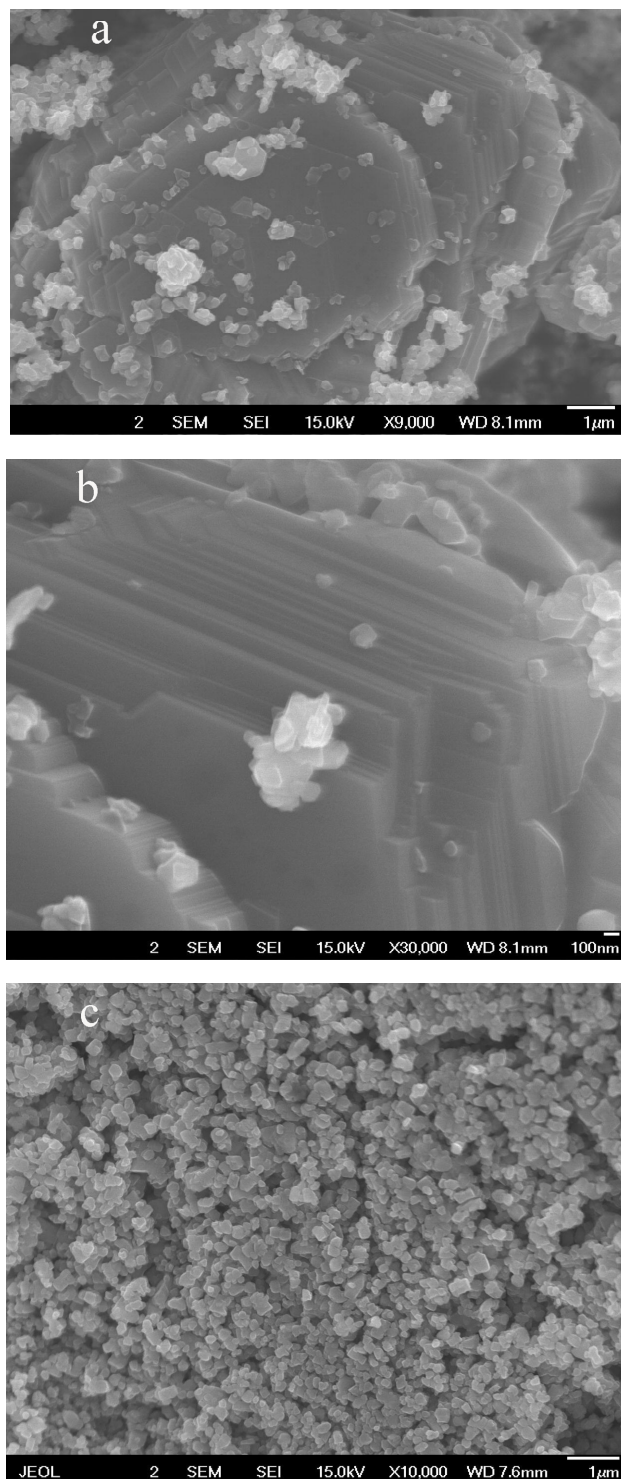


Figure 3. (a) and (b) SEM images of the laminated LiCoO₂ powder at different magnifications. (c) The image of the laminated LiCoO₂ powder ground in mortar.

electrochemical performance. The better electrochemical performance may be attributed to the facilitation of the insertion and deinsertion of lithium ions during the charge and discharge process

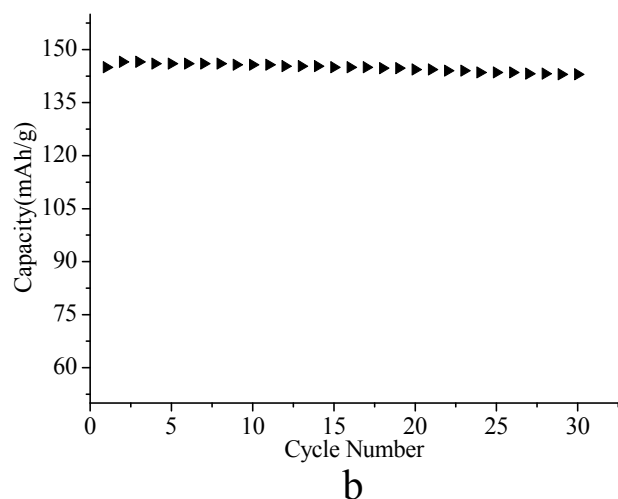
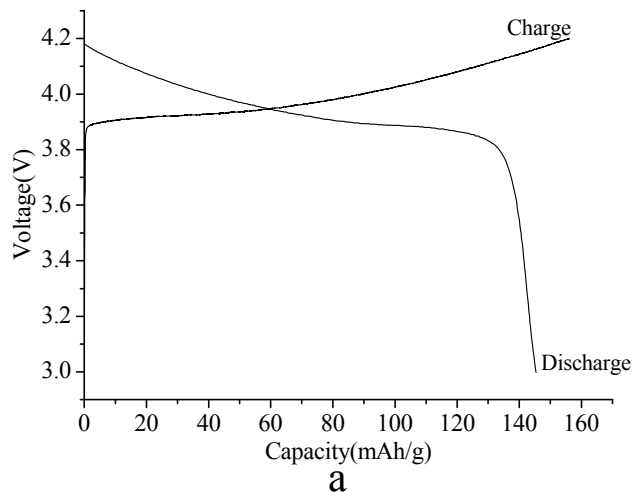


Figure 4. The cycling performance of of a button cell with the laminated LiCoO_2 as the cathode material (a) Initial discharge curve operated at 0.2C rate at 25°C. (b) The cycling profiles operated at 0.2C rate at 25°C.

[23-24]. Therefore we expect a better electrochemical performance of the synthesized laminated material after trituration due to the small size and even distribution of the particles.

3.4. Electrochemical properties

The initial charge/discharge curve of the laminated LiCoO_2 cathode is shown in Figure 4a. The electrode was cycled in the voltage range of 3.0–4.2 V at a constant current density of 0.2C rate at 25°C ($1\text{C} = 140\text{mAh}\cdot\text{g}^{-1}$). In the first cycle, the charge and discharge capacities are $156\text{mAh}\cdot\text{g}^{-1}$ and $145\text{mAh}\cdot\text{g}^{-1}$, respectively, and the coulombic efficiency is 93%. In order to determine the cyclability of the laminated LiCoO_2 cathode material, a cell was tested for 30 cycles. Figure 4b shows the results of the cycling test. The discharge capacity on the 30th cycle is $143\text{mAh}\cdot\text{g}^{-1}$. The capacity retention at the 30th cycle is 99%. These results demonstrate that the laminated LiCoO_2 cathode material has an excellent charge/discharge performance and a stable cyclability.

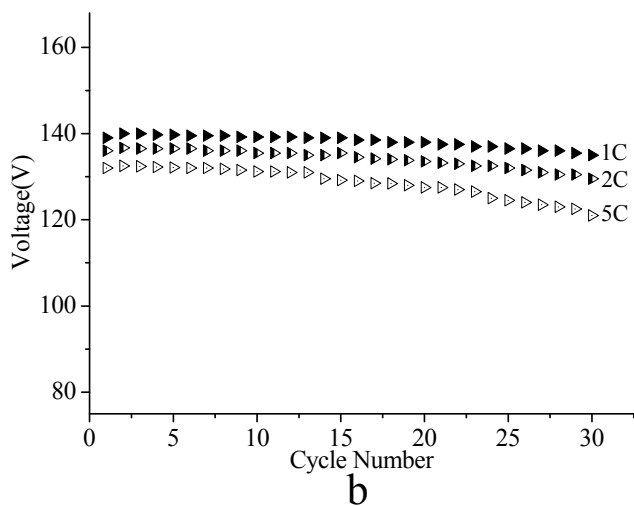
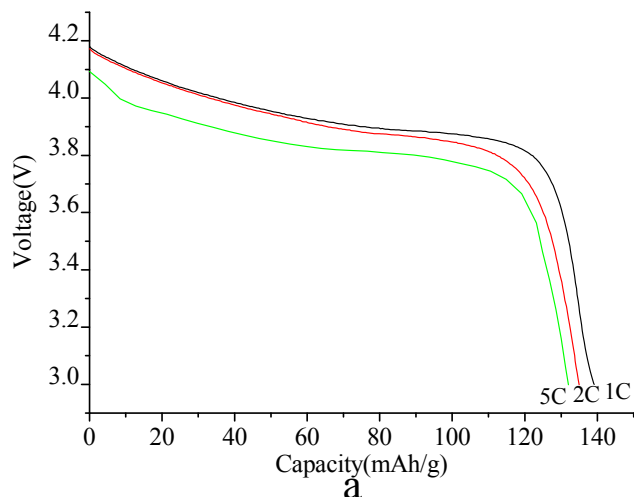


Figure 5. The cycling performance of of a button cell with the laminated LiCoO_2 as the cathode material (a) Initial discharge curves at 1C, 2C and 5C rates, respectively, at 25°C (b) The cycling profiles operated at 1C, 2C and 5C rates, respectively, at 25°C.

In order to evaluate the electrochemical property of the laminated LiCoO_2 material, the sample was charged and discharged at various rates of 1C, 2C, and 5C between 3 and 4.2V up to 30 cycles. A constant voltage (4.2V) was applied to each testing cell until the current decreased to 1/10th of its initial value during the charging process. Figure 5a shows the initial discharge curves of the sample at various rates. As shown in Figure 5a, the first discharge capacities are $139\text{mAh}\cdot\text{g}^{-1}$, $136\text{mAh}\cdot\text{g}^{-1}$ and $132\text{mAh}\cdot\text{g}^{-1}$ at 1C, 2C and 5C, respectively. Figure 5b shows the cycling discharge curves of the sample at various rates. After 30 cycles the discharge capacities of the cell cycled still maintain about $135\text{mAh}\cdot\text{g}^{-1}$, $128\text{mAh}\cdot\text{g}^{-1}$, and $120\text{mAh}\cdot\text{g}^{-1}$ for 1C, 2C and 5C rates, respectively. At the 30th cycle the capacity retentions are about 97%, 94% and 91% for 1C, 2C and 5C rates, respectively. These data show that the rate discharge performance and cycleability of the laminated LiCoO_2 powders are higher than that of Pt-doped LiCoO_2 based electrode as

reported by K. Du et al[25]. These results confirmed that the laminated LiCoO₂ powders have an excellent charge-discharge and cyclic performance, which may be ascribed to the highly ordered layered structure and nano-crystals of the LiCoO₂ powder[26]. However, further investigation is needed to elucidate the mechanism.

4. CONCLUSIONS

In this paper, the LiCoO₂ precursor was prepared using coprecipitation method. By mixing with LiNO₃ laminated LiCoO₂ cathode material was synthesized through three-stage temperature control. The morphologies of the synthesized LiCoO₂ powder clearly exhibit a well-ordered layered structure of the material. The laminated material has demonstrated an excellent discharge capacity and cycling performance. The initial discharge capacity is 145mAh·g⁻¹ (at 0.2C) with an excellent capacity retention of more than 99% after 30 cycles. The initial discharge capacities are 139mAh·g⁻¹, 136mAh·g⁻¹ and 132mAh·g⁻¹ at 1C, 2C and 5C, respectively, demonstrating an excellent charge/discharge performance at high currents. It is expected that the laminated LiCoO₂ powders can be served as promising cathode material for lithium rechargeable batteries. However, further investigation is needed to elucidate the mechanism.

5. ACKNOWLEDGEMENTS

This work is financially supported by the Natural Science Foundation of China under approval No. 20671031.

REFERENCES

- [1] J. G. Lee, T. G. Kim, B. Park, Mater. Res. Bull., 42, 1201 (2007).
- [2] C. L. Liao, Y. H. Lee, K. Z. Fung, J. Alloys Compd., 436, 303 (2007).
- [3] M. Matsui, K. Dokko, K. Kanamura, J. Power Sources, 177, 184 (2008).
- [4] Y. M. Lee, D. H. Ko, J. Y. Lee, J. K. Park, Electrochim. Acta, 52, 1582 (2006).
- [5] T. Fang, J. G. Duh, Surf.Coat.Technol., 201, 1886 (2006).
- [6] J. N. Reimers, J. R. Dahn, J. Electrochem. Soc., 139, 2091 (1992).
- [7] Y. K. Sun, I. H. Oh, S. A. Hong, J. Mater. Sci., 31, 3617 (1996).
- [8] M. Tabuchi, K. Ado, H. Kobayashi, H. Sakaebe, H. Kageyama, C. Masquelier, M. Yonemura, A. J. Hirano, Mater. Chem., 9, 199 (1999).
- [9] C. H. Han, P. Y. Yeh, J. Mater. Chem., 10, 599 (2000).
- [10] J. Ying, C. Jiang, C. Wan, J. Power Sources, 129, 264 (2004).
- [11] N. Li, C. J. Patrissi, G. Che, C. R. Martin, J. Electrochem. Soc., 147, 2044 (2000).
- [12] Y. X. Gu, D. R. Chen, X. L. Jiao, J. Phys. Chem B, 109, 17901 (2005).
- [13] H. Wang, Y.-H. Jang, B. Huang, D. R. Sadoway, Y.-M. Chiang, J. Electrochem. Soc., 146, 473 (1999).
- [14] S. M. Lala, L. A. Montoro, J. M. Rosolen, J. Power Sources, 124, 118 (2003).
- [15] T. Kawamura, M. Makidera, S. Okada, J. I. Yamaki, J. Power Sources, 146, 27 (2005).
- [16] Anjuli T. Appapillai, Azzam N. Mansour, Jaephil Cho, Yang Shao-Horn, Chem. Mater., 19, 5748 (2007).
- [17] W. J. Clegg, K. Kendall, N. M. Alford, Nature, 347, 445 (1990).
- [18] A. Rougier, P. Gravereau, C. Delmas, J. Electrochem. Soc., 143, 1168 (1996).
- [19] R. J. Gummow, M. M. Thackeray, W. I. F. David, Res. Bull., 27, 317 (1992).
- [20] S. T. Myung, N. Kumagai, S. Komaba, H. T. Chung, J. Appl. Electrochem., 30, 1081 (2000).
- [21] J. R. Dahn, U. von Sacken, C. A. Michal, Solid State Ionics, 44, 87 (1990).
- [22] J. N. Reimers, E. Rossen, C. D. Jones, J. R. Dahn, Solid State Ionics, 61, 335 (1993).
- [23] M. J. Zou, M. Yoshio, S. Gopukumar, J. I. Yamaki, Electrochem. Solid State Lett., 7, A176 (2004).
- [24] K. M. Shaju, G. V. Subba Rao and B. V. R. Chowdari, Electrochim. Acta, 48, 145 (2002).
- [25] K. Du, H. Zhang, L. Qi, Electrochimica Acta, 50, 211 (2004).
- [26] M. K. Jo, Y. S. Hong, J. B. Choo, J. P. Cho, J. Electrochemical Society, 156, A430 (2009).

